ROCKY MOUNTAIN
JOURNAL OF MATHEMATICS
Volume 8, Numbers 1 and 2,
Winter and Spring 1978

APPLICATIONS OF THE INVERSE SCATTERING TRANSFORM I: SELF-INDUCED TRANSPARENCY*

D. J. KAUP

ABSTRACT. By using some of the more important, but simple consequences of the inverse scattering transform, we show how a relatively large amount of information concerning the solution can be obtained. Using self-induced transparency as an example, we show how the McCall-Hahn area theorem, nonlinear moments, and nonlinear transmission are related to the scattering data, and how the final soliton configuration is related to the initial pulse profile.

One of the major difficulties with the inverse scattering method has been the apparently complicated nature of the inverse scattering transform. Concerning this, we wish to make two points. First, the derivation of the Marchenko equations used in the inversion procedure may well be complicated, but we remind the reader that the same is also true for a rigorous proof of the Fourier inversion procedure. Second, without even using the inversion procedure, or the Marchenko equations, there is still a considerable amount of information which can be gleaned by using only the direct scattering problem. In other words, we can do inverse scattering without using inverse scattering! We will illustrate this with two examples: self-induced transparency (SIT) and the three-wave resonant interaction (3WRI). In this paper, we shall treat SIT, and in the following paper, 3WRI. In our presentation, one should note that nowhere shall we use those "complicated" inverse scattering equations. Instead, we shall use only their more important consequences.

The phenomenon known as self-induced transparency (SIT) was first described by McCall and Hahn [1], [2], who found that they could explain the observed phenomena in terms of the following simple model. Consider an electromagnetic pulse incident onto a two-level atom, where the central frequency of the pulse matches the resonant frequency of the two-level atom. Let us say that the pulse is sufficiently strong so that it will excite all of the atoms in the first layer of the material from the ground state into the upper level, as illustrated in Figure 1a, b.

Then the second half of the pulse will move forward and impress a strong electric field onto these atoms (Figure 1c). This will stimulate

*Research supported in part by the National Science Foundation.

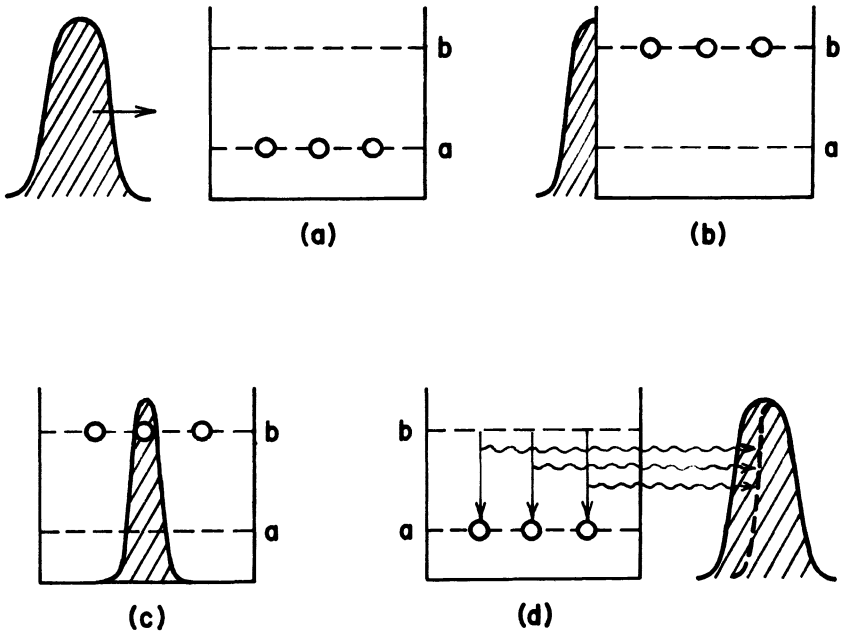

Figure 1. Schematic manner by which lossless propagation occurs. In (a), the electromagnetic pulse is approaching three atoms in their ground state. In (b), the first half of the pulse is absorbed by the atoms, sending them into their excited states. In (c), the last half of the pulse is impressed on the excited atoms, stimulating them to decay back into the ground state as shown in (d), with the emitted energy being added coherently onto the tail of the second half of the original pulse.

them into returning to the ground state; in the process, they will emit *coherently* the first half of the pulse, which was absorbed. Now this half is added to the rear of the second half of the pulse, as illustrated in Figure 1d. The net result of this has been to move the pulse through the first layer of atoms, without any energy loss, although with a reduced velocity. This process repeats itself as the pulse propagates through the medium, in such a manner that the material appears to be transparent to this pulse.

If the pulse is not of the right shape, this will not happen. For example, if it is too small, most of the pulse will be expended in exciting the atoms, and not enough will be left over to completely stimulate all of the atoms into returning to the ground state. Thus energy will be lost by the pulse, and it will eventually be completely absorbed. On the other hand, if the pulse is a little larger, it will still cycle as indicated in Figure 1, but now the last half of the pulse will be too strong, which

will send some of the atoms back up into the excited state. Again energy is lost, but on the next cycle it will have become closer to the required shape for lossless propagation.

For larger pulses, one can have sufficient pulse energy to create even two or more cycles. After the pulse has been given sufficient strength to create at least one cycle, one finds that the majority of the pulse energy is propagated losslessly, and the transmission coefficient becomes relatively large (close to unity). This phenomenon, which we shall discuss more fully later, is known as "nonlinear transmission" [2], [3].

One of the best known results of McCall and Hahn is their "area theorem" [2],

$$\frac{d\theta(z)}{dz} = -\frac{1}{2}\alpha \sin \theta(z), \tag{1}$$

where

$$\theta(z) = \int_{-\infty}^{\infty} \epsilon(z, t)\, dt, \tag{2}$$

ϵ is the (real) electric field envelope, z is the propagation direction of the plane pulse, and α is the inverse Beer length. It is this area, $\theta(z)$, which determines how many times the atoms cycle between the ground state and the excited state. When the area is between zero and π, (1) shows that it must monotonically approach zero, when between π and 3π, it approaches 2π, which corresponds to one cycle, etc. Due to this changing area as the pulse propagates, a pulse reshaping occurs as well as a pulse breakup, where the original pulse breaks up into individual pulses, each of area 2π, and each with a different propagation velocity. These effects have been observed experimentally, the most accurate study being that of Slusher and Gibbs [3]. In particular, they have compared computer simulations with their experimental results, and they have found excellent agreement.

The development of the inverse scattering theory for self-induced transparency was pioneered by Lamb [4, 5, 6], the Manchester group found N-soliton solutions [7, 8, 9], Lamb deduced the correct eigenvalue problem and described the soliton spectrum [5, 6], and finally, Ablowitz, Kaup, and Newell [10] solved the complete problem, including the continuous spectrum. It was only with the latter result that one could finally see how these previous results were related to the initial data and the scattering data.

Let's start with the McCall-Hahn area theorem. Recall that the area is just the linear Fourier transform evaluated at zero wavevector. Since the reflection coefficient, $\bar{b}(\zeta)$, is like a nonlinear Fourier transform, it

should not then be surprising that $\bar{b}(0)$ is also related to the area. To show this, we start with the Zakharov-Shabat equation as suggested by Lamb [5],

$$\phi_{1\tau} + i\zeta\phi_1 = \tfrac{1}{2}\epsilon\phi_2, \tag{3a}$$

$$\phi_{2\tau} - i\zeta\phi_2 = -\tfrac{1}{2}\epsilon^*\phi_1, \tag{3b}$$

where $\tau = t - z/c$ and $\chi = z$ are our new coordinates. Although Professor Newell's paper has discussed this equation and its scattering data more thoroughly, we shall simply review the essential features. The solution ϕ of (3) is determined by the boundary condition $\phi \to \binom{1}{0} e^{-i\zeta\tau}$ as $\tau \to -\infty$. Then as $\tau \to +\infty$,

$$\phi \to \begin{pmatrix} ae^{-i\zeta\tau} \\ be^{i\zeta\tau} \end{pmatrix}$$

where $a(\zeta)$ is the "transmission coefficient" and $b(\zeta)$ is the "reflection coefficient." The zeros of $a(\zeta)$ in the upper half ζ-plane give us the bound state spectrum. The other reflection coefficient $\bar{b}$, connected with plane waves incident from $+\infty$, is given in this case by $\bar{b}(\zeta) = b^*(\zeta^*)$.

Returning to the problem at hand, we want the soluton ϕ of (3) for $\zeta = 0$, and since the McCall-Hahn area theorem is only valid for ϵ real, we also require the same. The solution with the appropriate boundary condition [11] on ϕ is then

$$\phi = \begin{pmatrix} \cos\frac{1}{2}\mathscr{A} \\ -\sin\frac{1}{2}\mathscr{A} \end{pmatrix}, \tag{4}$$

where

$$\mathscr{A} \equiv \int_{-\infty}^{\tau} \epsilon\, d\tau. \tag{5}$$

Thus, it follows [11] that

$$a(\zeta = 0) = \cos\tfrac{1}{2}\theta, \tag{6a}$$

$$\bar{b}(\zeta = 0) = -\sin\tfrac{1}{2}\theta, \tag{6b}$$

where θ is given by (2). Now, from the complete solution [10], it also follows that

$$\partial_\chi \ln\left(\frac{\bar{b}}{a}\ (\zeta = 0)\right) = -\frac{1}{2}\alpha, \tag{7}$$

where α is the inverse Beer length and χ is the distance in the direction of propagation. Thus, from (6) and (7),

$$\partial_\chi \ln \tan \tfrac{1}{2}\theta = -\tfrac{1}{2}\alpha, \tag{8}$$

which is identical to (1). Of course, one need not stop here. In the same way that the *linear first moment* is related to the derivative of the Fourier transform at zero argument, we also find a "nonlinear" first moment [12]. When the envelope has a total area of zero ($\theta = 0$), it is given by

$$\mu_1 = \int_{-\infty}^{\infty} d\tau\, \tau\epsilon \cos\mathscr{A}, \tag{9}$$

and also evolves according to

$$\partial_\chi \ln \mu_1 = -\tfrac{1}{2}\alpha. \tag{10}$$

Thus, like $\tan\frac{1}{2}\theta$ for $\theta \neq 0$, this nonlinear first moment, μ_1, for $\theta = 0$ must also approach zero as the pulse evolves.

Let's return to the nonlinear transmission of the pulse energy. We have a nonlinear Parseval relation, which follows from the infinity of conserved quantities [11], [13], and is given by

$$\begin{aligned}\frac{1}{8}\int_{-\infty}^{\infty} \epsilon^*\epsilon\, d\tau &= 2\sum_{j=1}^{J}\eta_j \\ &\quad + \frac{1}{2\pi}\int_{-\infty}^{\infty}\ln[1+\Gamma(\xi,\chi)]\,d\xi,\end{aligned} \tag{11}$$

where $[\eta_j]_{j=1}^{J}$ are the imaginary parts of the bound state eigenvalues, and $\Gamma(\xi, \chi)$ is defined by

$$\Gamma(\xi, \chi) \equiv |\bar{b}/a(\xi, \chi)|^2. \tag{12}$$

Note that for very small fields, since $\bar{b}/a$ is just the linear Fourier transform of ϵ, [11], we have $\Gamma \ll 1$, and (11) becomes the ordinary Parseval relation (since $J = 0$). In the fully nonlinear case, from the complete solution [10], we have

$$\Gamma(\xi, \chi) = \Gamma(\xi, 0)e^{-\pi g(2\xi)\chi} \tag{13}$$

where $g(2\xi)$ is the inhomogeneous broadening factor. Thus, for sufficiently large χ, Γ vanishes, leaving only the soliton part in (11) which is transmitted losslessly. Thus the radiation is absorbed and it is the solitons which propagate losslessly.

To see how these components compare in their energy content, let the initial profile be a box, such as

$$\epsilon(\tau) = \begin{cases} E \text{ if } 0 < \tau < \tau_p \\ 0 \text{ otherwise} \end{cases}, \tag{14}$$

for which the initial area is

$$\theta_0 = E\tau_p. \tag{15}$$

Define

$$T(\chi) \equiv \frac{\tau_p}{8} \int_{-\infty}^{\infty} \epsilon^* \epsilon \, d\tau, \tag{16}$$

which is proportional to the energy of the pulse. Then at $\chi = 0$,

$$T(0) = \tfrac{1}{8}\theta_0^2, \tag{17}$$

and as $\chi \to +\infty$, from (11),

$$T(\infty) = 2 \sum_{j=1}^{J} (\eta_j \tau_p). \tag{18}$$

In Figure 2, we have plotted the various parts as a function of θ_0. Looking at this figure, the first thing one notices is that after being consistent with the area theorem, as much of the initial energy as practical goes into the solitons, leaving the continuous spectrum, or radiation, with only the small cross-hatched part. Of course, for small energies where θ_0 is less than π, all of the incident energy is radiation energy, which is absorbed by the medium. But as θ_0 increases, crosses π (and every odd integer multiple of π) an additional soliton is allowed, and is formed. The solitons then take up a larger and larger fraction of the incident energy as the initial area increases. Of course, if instead we have plotted the ratio of the transmitted energy (solitons) to the incident energy, we would have obtained a plot similar to Figure 13 in [3]. But, as plotted in our Figure 2, one can see more clearly how the incident energy is distributed between the various solitons and the radiation.

Let us now turn our attention to how one determines the configuration of the final state ($\chi \to \infty$). In this limit, the radiation part vanishes when one is away from the light cone [**10**], and the only significant remaining part is the soliton part. To determine this part of the solution, we only need to know the bound state eigenvalues $[\zeta_j]_{j=1}^J$ and the normalization constants $[D_j]_{j=1}^J$ [**5**], [**10**]. There are four basic methods that one could use to determine these quantities:

A. Numerically integrate the Maxwell-Bloch partial differential equations directly.

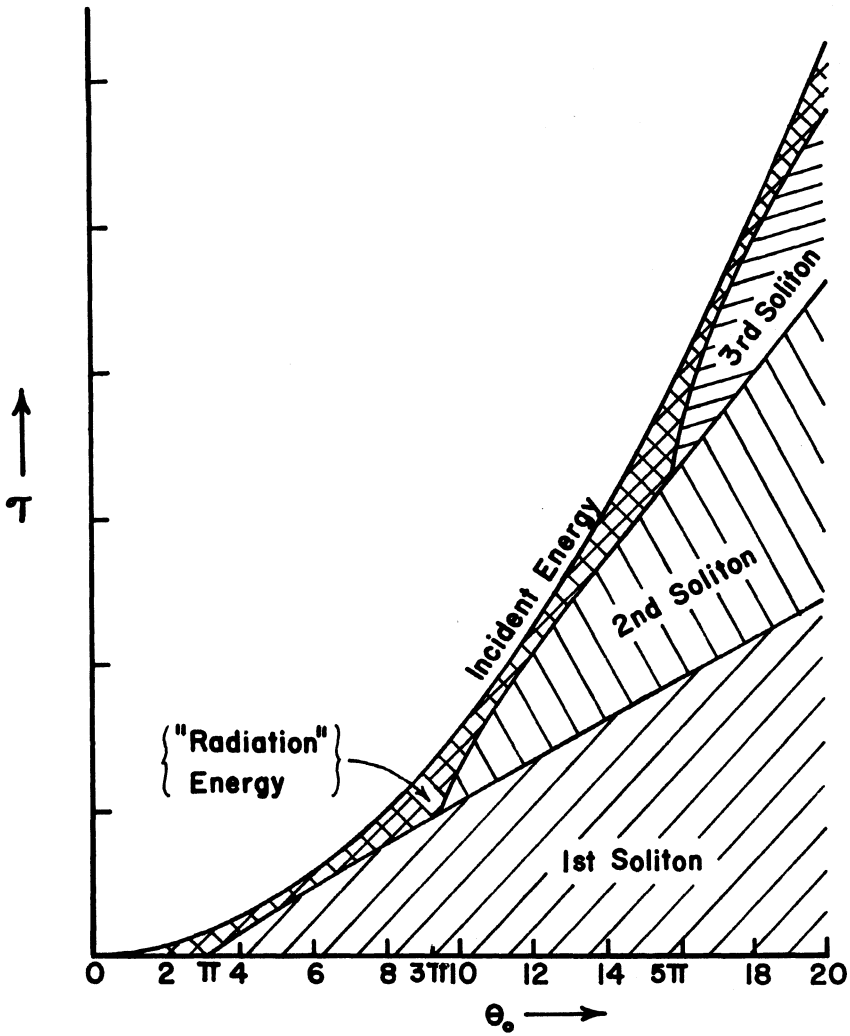

Figure 2. The relative distribution of the initial energy among the various solitons and the radiation, as a function of initial area, θ_0, for the box profile described in the text.

B. Use the infinity of conserved quantities.

C. Numerically solve for the eigenvalues of the Zakharov-Shabat equations.

D. Use the WKB approximation to find approximate eigenvalues for the Zakharov-Shabat equation.

Method A was the first used [1], [2], [3], is accurate, but at the same time is very time consuming, without giving one a general feeling for how the eigenvalue spectrum is related to the initial profile. Method B as developed [13], [14], [15] involves an approximation wherein one effectively ignores the radiation part of the initial profile. After glancing at Figure 2, one can see why this approximation works so well when θ_0 is not close to an odd integer multiple of π, because the radiation amount is then relatively small when $\theta_0 > \pi$. But due to neglecting the radiation, this method cannot give the correct threshold values of $\theta_0 = (2n + 1)\pi$.

Like method A, method C is exact, but is much faster, in that one is only solving for the eigenvalues of an ordinary differential equation. Examples of results for this method are shown as solid lines in Figures 3–5 for the three initial profiles given by

$$\epsilon(0, \tau) = \begin{cases} \theta_0/\tau_p \text{ if } 0 < \tau < \tau_p \\ 0 \text{ otherwise,} \end{cases} \tag{19a}$$

$$\epsilon(0, \tau) = \begin{cases} \dfrac{16\theta_0}{\tau_p^2}\tau e^{-4\tau/\tau_p} & \text{if } 0 < \tau \\ 0 & \text{if } 0 > \tau, \end{cases} \tag{19b}$$

$$\epsilon(0, \tau) = \frac{\theta_0 2^{1/2}}{\tau_p} e^{-2\pi\tau^2/\tau_p^2}. \tag{19c}$$

Method D uses the WKB approximation, which is valid for real, slowly varying profiles with only a single extremum. When these conditions are satisfied, we have

$$\int_a^b \sqrt{\tfrac{1}{4}\epsilon^*\epsilon - \eta_j^2}\; d\tau = \pi(2j - 1), \tag{20}$$

as giving approximate values [16] of the imaginary part of the eigenvalues, $[\eta_j]_{j=1}^J$, where a and b are the classical turning points. This method has the advantage over method B in that it does give the *exact* threshold values of $\theta_0 = (2n + 1)\pi$. The WKB solutions for the three initial profiles given by (19) are shown also in Figures 3–5, but as dashed lines. One should note that this approximation is the worst for the box, which is not slowly varying at the edges, is better for the $\tau e^{-\tau}$ profile, which has only a discontinuity in the slope at $\tau = 0$, and is very good for the Gaussian, which is indeed slowly varying.

In summary, we want to emphasize that none of these results involved solving tthe inverse scattering (Marchenko) equations. All of these results were obtained by simpler means. From a knowledge of the

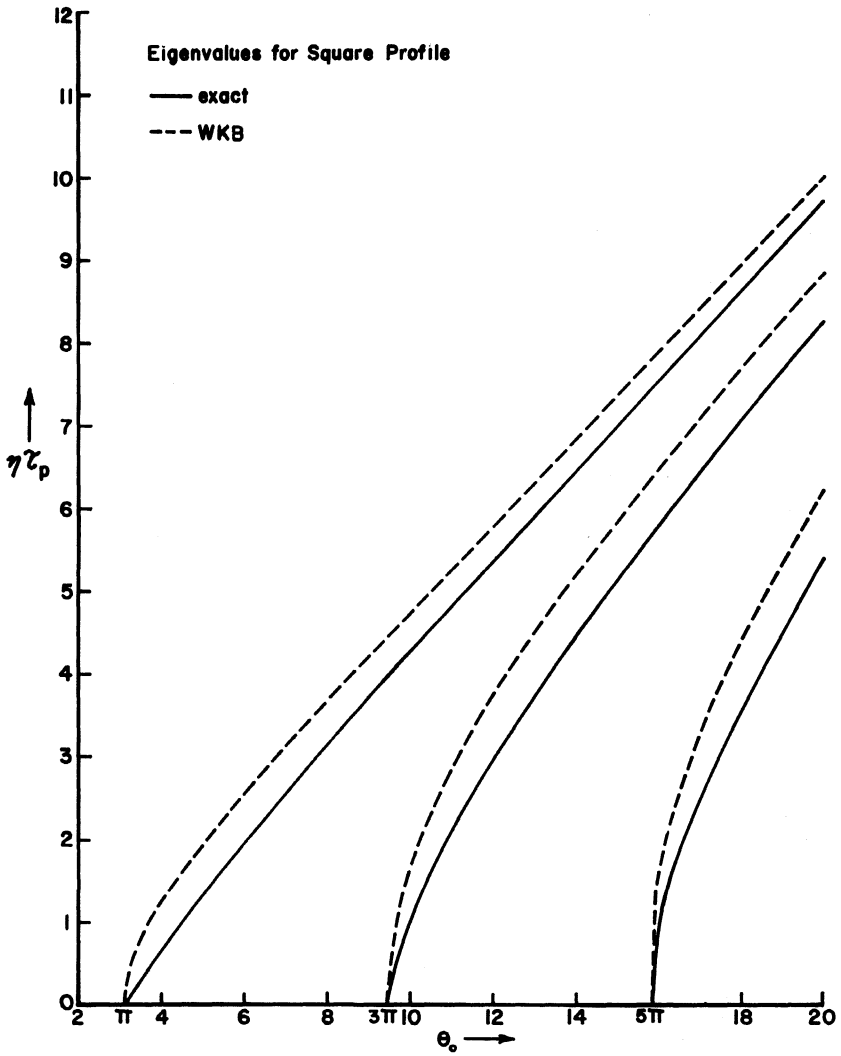

Figure 3. Exact bound state eigenvalues and the corresponding WKB values as a function of θ_0 for the box profile discussed in the text.

scattering data in the neighborhood of $\zeta = 0$, we can obtain the areas and all higher nonlinear moments of the pulse. From a knowledge of $\Gamma(\zeta)$ for real ζ, we can determine the energy of a pulse, as well as all of the higher infinity of conserved quantities. From knowing the initial profile, we can determine all of the eigenvalues (as well as all of the

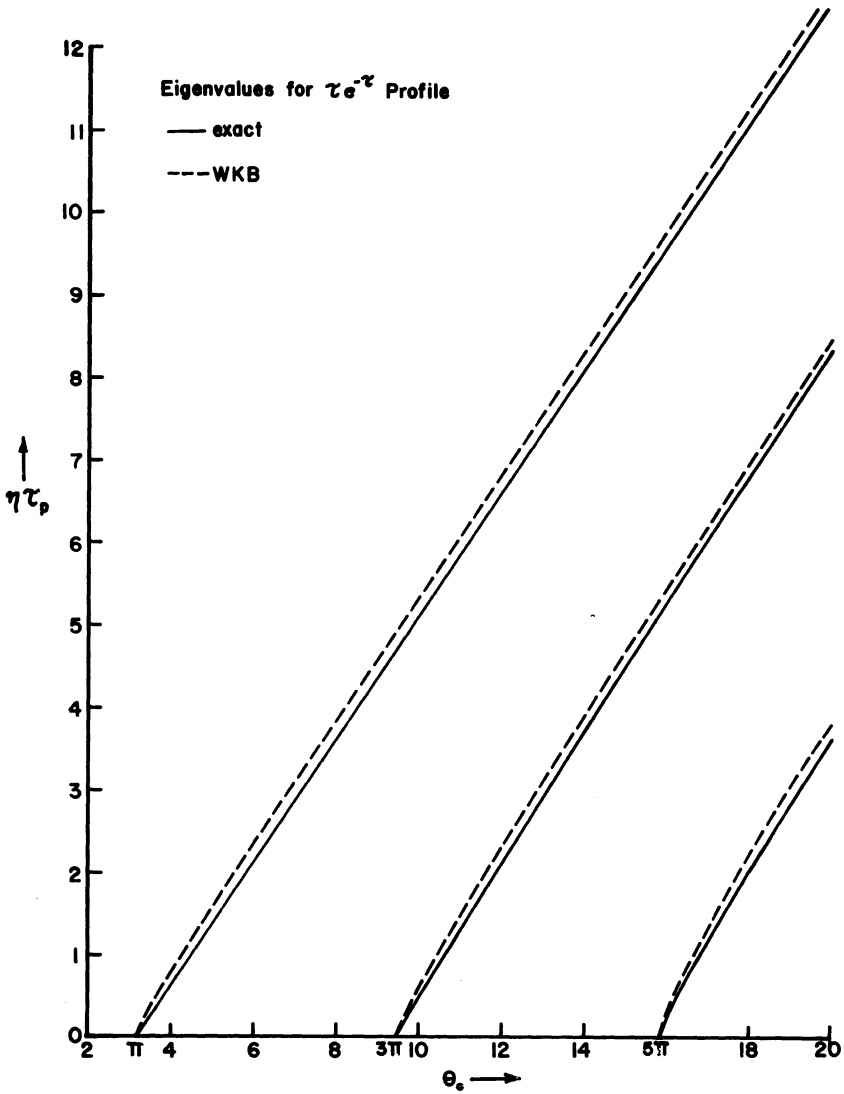

Figure 4. Exact bound state eigenvalues and the corresponding WKB values as a function of θ_0 for the $\tau e^{-\tau}$ profile discussed in the text.

normalization coefficients), from which one can construct the final soliton state. And with only this, one already has a very good feel for what the solution of the inverse scattering equations should be.

The author is indebted to Professor A. C. Newell for pointing out the relation between b/a and the area developed above.

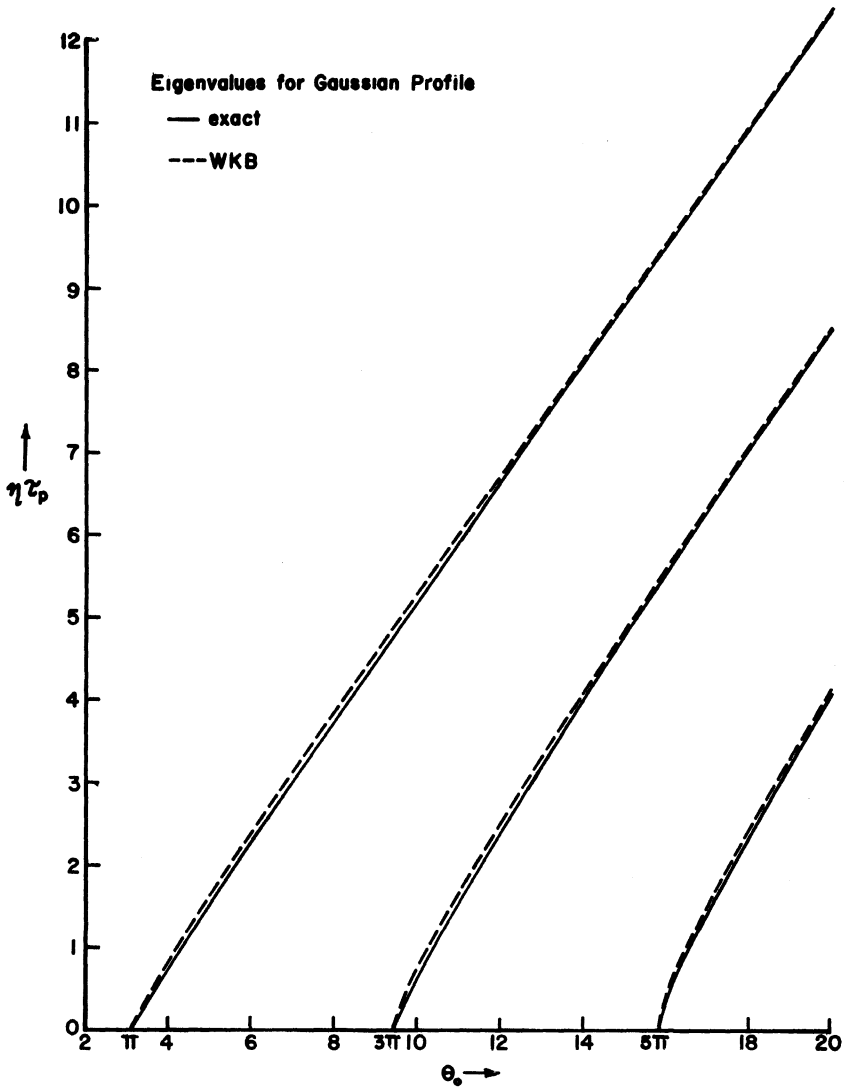

Figure 5. Exact bound state eigenvalues and the corresponding WKB values as a function of θ_0 for the Gaussian profile discussed in the text.

References

1. S. L. McCall and E. L. Hahn, *Self induced transparency by pulsed coherent light,* Phys. Rev. Lett. **18** (1967), 908–911.

2. ———, *Self-induced transparency,* Phys. Rev. **183** (1969), 457–485.

3. R. E. Slusher and H. M. Gibbs, *Self induced transparency in atomic rubidium,* Phys. Rev. **A5** (1972), 1634–1659. *Erratum in Phys. Rev.* **A6** (1972), 1255–1257.

4. G. L. Lamb, Jr., *On the connection between lossless propagation and pulse profile,* Physica **66** (1973), 298–314.

5. ———, *Phase variation in coherent-optical-pulse propagation,* Phys. Rev. Lett. **31** (1973), 196–199.

6. *Coherent-optical-pulse propagation as an inverse problem,* Phys. Rev. **A9** (1974), 422–430.

7. P. J. Caudrey, J. D. Gibbon, J. C. Eilbeck, and R. K. Bullough, *Exact multisoliton solutions of the self-induced transparency and sine-Gordon equations,* Phys. Rev. Lett. **30** (1973), 237–238.

8. J. C. Eilbeck, J. D. Gibbon, P. J. Caudrey, and R. K. Bullough, *Solitons in nonlinear optics. I. A more accurate description of the* 2π *pulse in self-induced transparency,* J. Phys. **A6** (1973), 1337–1347.

9. J. D. Gibbon, P. J. Caudrey, R. K. Bullough, and J. C. Eilbeck, *An N-soliton solution of a nonlinear optics equation derived by a general inverse method,* Lett. Nuovo Cimento **8** (1973), 775–779.

10. M. J. Ablowitz, D. J. Kaup, and A. C. Newell, *Coerent pulse propagation, a dispersive irreversible phenomenon,* J. Math. Phys. **15** (1974), 1852–1858.

11. M. J. Ablowitz, D. J. Kaup, A. C. Newell, and H. Segur, *The inverse scattering transform-Fourier analysis for nonlinear problems,* Stud. Appl. Math. **53** (1974), 249–315.

12. D. J. Kaup (to be published).

13. G. L. Lamb, Jr., M. O. Scully, and F. A. Hopf, *Higher conservation laws for coherent optical pulse propagation in an inhomogeneously broadened medium,* Appl. Opt. **11** (1972), 2572–2575.

14. D. D. Schnack and G. L. Lamb, Jr., *Higher conservation laws and coherent pulse propagation,* Coherence and Quantum Optics, L. Mandel and E. Wolf, eds., Plenum Press, New York, 1973, pp. 23–33.

15. R. T. Deck and G. L. Lamb, Jr., *Phase variation in coherent-optical-pulse propagation,* Phys. Rev. **A12** (1975), 1503–1512.

16. V. E. Zakharov and A. B. Shabat, *Exact theory of two-dimensional self-focusing and one-dimensional self-modulation of waves in nonlinear media,* Sov. Phys. JETP **34** (1972), 62–69.

DEPARTMENT OF PHYSICS, CLARKSON COLLEGE OF TECHNOLOGY,
POTSDAM, NY 13676